ELECTRONIC AUTORADIOGRAPHY OF LIVING HUMAN CELLS WITH A MWPC

R. BELLAZZINI [1,2], G. BETTI [1], A. DEL GUERRA [1,2], M.M. MASSAI [1,2],
M. RAGADINI [1,2], G. SPANDRE [1,2], G. TONELLI [1,2] and R. VENTURI [3]

[1] Istituto di Fisica dell'Università, Piazza Torricelli, 2, I-56100 Pisa, Italy
[2] I.N.F.N., Istituto Nazionale di Fisica Nucleare, Sezione di Pisa, Via Livornese, San Piero a Grado, I-56010 Pisa, Italy
[3] C.N.R., Gruppo Nazionale di Elettronica Quantistica, Unità di Pisa, Piazza Torricelli, 2, I-56100 Pisa, Italy

The use of a multiwire proportional chamber (MWPC) for mapping the incorporation of a radioactive precursor of DNA biosynthesis by aggregates of cells is discussed. The resolving power, sensitivity and linearity of the developed system are shown, together with preliminary "electronic autoradiograms" of ^{14}C-labelled cells.

1. Introduction

The use of radioacive tracers has proved to be an extraordinarily useful tool in biological research. Subcellular structures have been resolved and the intimate mechanism of biological processes going on within the cell has been elucidated through studies based on the use of appropriate radiolabelled molecules.

The conventional techniques available to the biologist for the detection of radioactivity, such as photographic emulsion based autoradiography and liquid scintillation counting, are usually destructive of the biological sample under investigation. For many purposes, however, the rescue of living cells after the radioactivity measurement would be very helpful.

In a previous paper [1] we have shown that a MWPC could be used as an electronic autoradiography system when variations in the ability of cell clones and other cell aggregations to incorporate or attract radioactive precursors have to be studied. In particular, a non-selective method for the isolation of DNA repair deficient mutants in mammalian cells was discussed. The method requires radioactive labelling of the short DNA sequences synthesized during repair of damaged regions. Mutants should be recognized by the absence of radioactive incorporation into their DNA (for a more complete and general discussion on this subject, see ref. 1).

Here we present the results obtained with an "ad hoc" designed MWPC with optimized mechanical characteristics, improved read-out system and high sensitivity for the reconstruction of low level β^- activity maps. Tests performed with γ and β sources are discussed and actual autoradiograms of ^{14}C-labelled living cells are presented.

2. The MWPC and the read-out system

A crucial problem in localizing and identifying small, individual spots of β^- activity with gaseous detectors is connected with the range of the β^--rays inside the detector volume.

The spread-out of an isotropically β^- emitting source at a distance L from the detection plane and with extended (track) ionization can be approximately modelled, assuming rectilinear tracks and exponential attenuation, and neglecting the self-absorption in the source, by

$$\rho(r) = \frac{N_0}{2\pi}\left[\frac{1}{\lambda}\int_{L-L_0}^{L}\frac{\exp\left[-\frac{\sqrt{r^2+z^2}\,(2z-L^*)}{z\lambda}\right]}{r^2+z^2}\,dz\right.$$
$$\left.+\frac{1}{2L^2}\frac{\exp\left(-\frac{L_T}{\lambda}\sqrt{1+\frac{r^2}{L^2}}\right)}{\left(1+r^2/L^2\right)^{3/2}}\right],\qquad(1)$$

where N_0 is the number of emitted particles, λ the absorption coefficient, L_0 the cathode–anode distance, L_T the total absorption thickness (mylar window + gas) and $L^* = 2L - L_T$ (fig. 1). This equation gives the bidimensional density distribution of the center of gravity of the ionization clouds as a function of the distance from the source projected on the detection plane.

The first part of eq. (1) accounts for β^- particles ($\geq 30\%$ of total for ^{14}C) ending their ionization path inside the active volume of the detector, while the
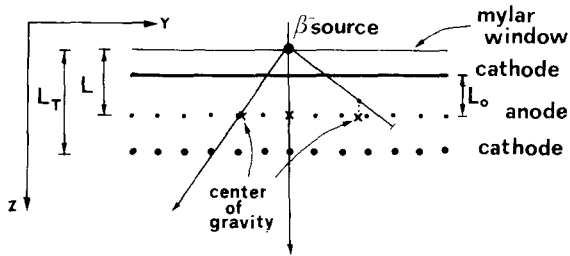
Fig. 1. Schematic drawing of the MWPC and of the source image spread-out.

second part accounts for particles ending outside.

The area of the source image, i.e. the area on which 50% of detected events are collected, is shown in fig. 2 as a function of the main MWPC design parameters.

To improve both resolving power and sensitivity of the detection system to ^{14}C-labelled cells we have then designed a MWPC with a very thin mylar window (9 μm), small anode–cathode gap (4 mm) and a minimized non active volume ($L - L_0 = 1$ mm). With this design one can obtain a transmission factor of about 70% for the ^{14}C β^- spectrum, a significant reduction in the spatial extension of the source image and a reasonable compromise with the requirement of detector mechanical and electrostatic stability.

Separation between adjacent wires is 2 mm and the total useful detection area is about 600 cm^2. To keep the cost of the associated electronic circuitry reasonably low we have chosen a cathode-coupled delay line read-out system with the anode signal only used as an ENABLE. The delay line and its characteristics have been fully described elsewhere [1]. The one-end start, the other-end stop technique has definite advantages with respect to
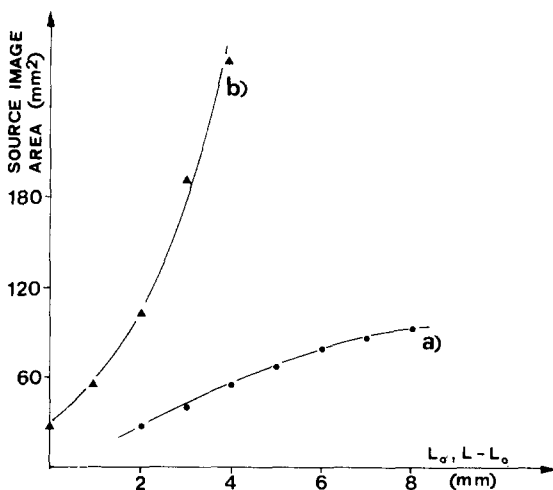

Fig. 2. The area of the source image as a function of: (a) gap-width (L_0) at $L - L_0 = 1$ mm, (b) source–cathode distance ($L - L_0$) at $L_0 = 4$ mm.
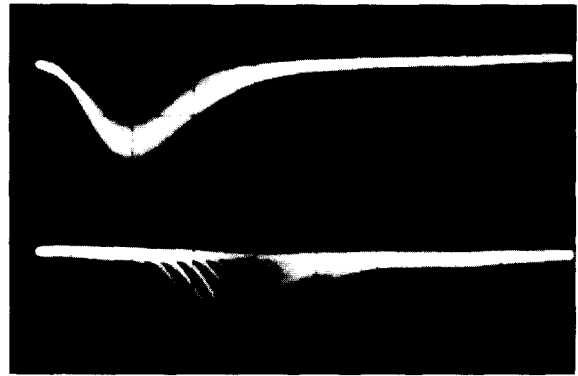

Fig. 3. One-end delay-line output signals (lower) triggered by the signal from the other end of the delay-line (upper). Horizontal scale is 100 ns/div.

the anode-start, one-end stop technique in improving the spatial resolution (doubling the relative delay of the two signals and thus doubling the specific delay per unit length), the linearity and the response uniformity (due to compensation effects along the delay-line). The pick-up and processing of the signals are obtained by means of low-noise, charge sensitive pre-amplifiers which also constitute the "cold" termination of the delay line. The differential and integral shaping constants of the subsequent timing filter amplifiers (TFA Ortec 454) are selected in order to optimize the signal-to-noise ratio (fig. 3). An accurate timing system based on constant fraction discrimination (CFD Ortec 583) is used to measure the time of arrival of the signals at both ends of the delay-line with accuracy better than 2 ns.

The processed signals from the two ends of each delay-line are the start and stop of two time to amplitude converters (TAC Ortec 467) that drive the x and y deflection plates of an oscilloscope; the z axis of the oscilloscope is intensified by the AND of the two TAC signals. A Polaroid camera is used as a permanent storage of the obtained analog information (fig. 4).

3. The MWPC performance

The intrinsic spatial resolution of the system has been measured irradiating the chamber with an uncollimated ^{55}Fe source (5.9 keV X-rays) and measuring only the y coordinate, orthogonal to the anode wires. In this configuration the source may be considered as localized within a narrow spot around the sense wire so that the problems related to the finite dimensions of the source can be neglected. Fig. 5 shows the arrival time distribution of the output signals at one end of the delay-line, when the start is given by the output signal fom the other end. The arrival time distribution from a single wire has a fwhm of 400μm, and the correspond-
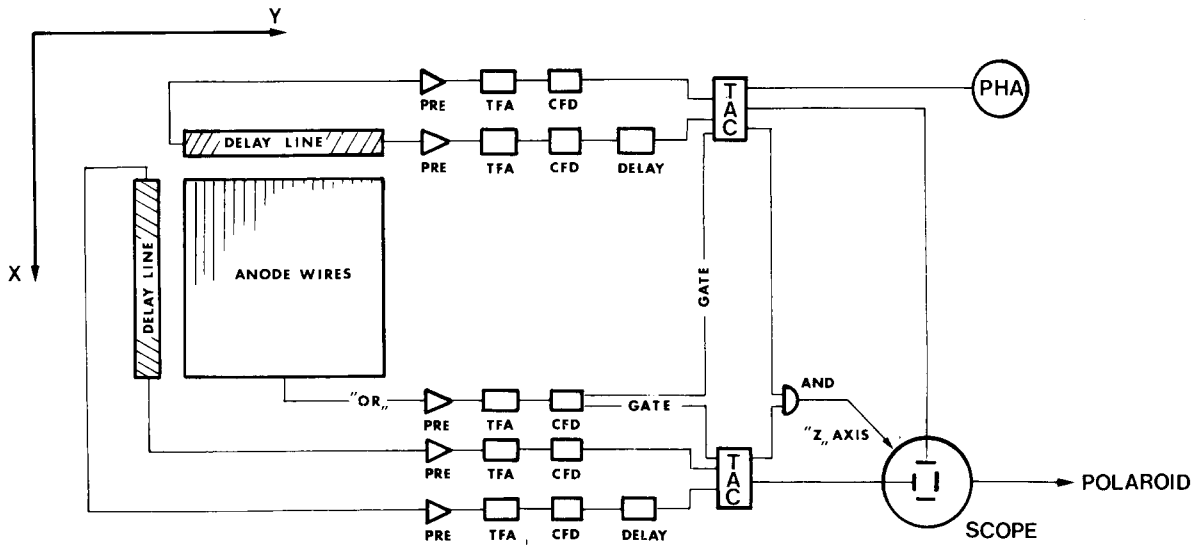
Fig. 4. Schematic drawing of the electronics and read-out system.
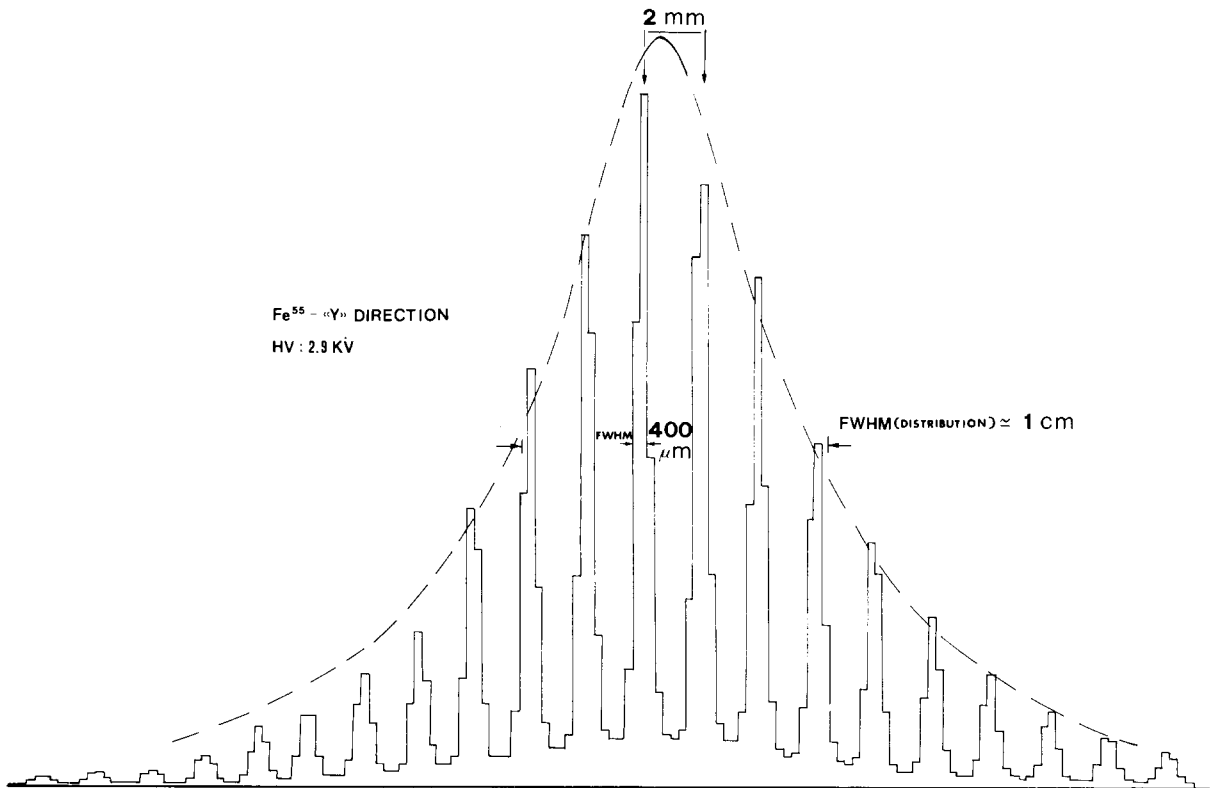
Fig. 5. Intrinsic spatial resolution as measured with an ^{55}Fe source: full line, measured discretized distribution; dashed line, calculated continuous distribution (see also text).
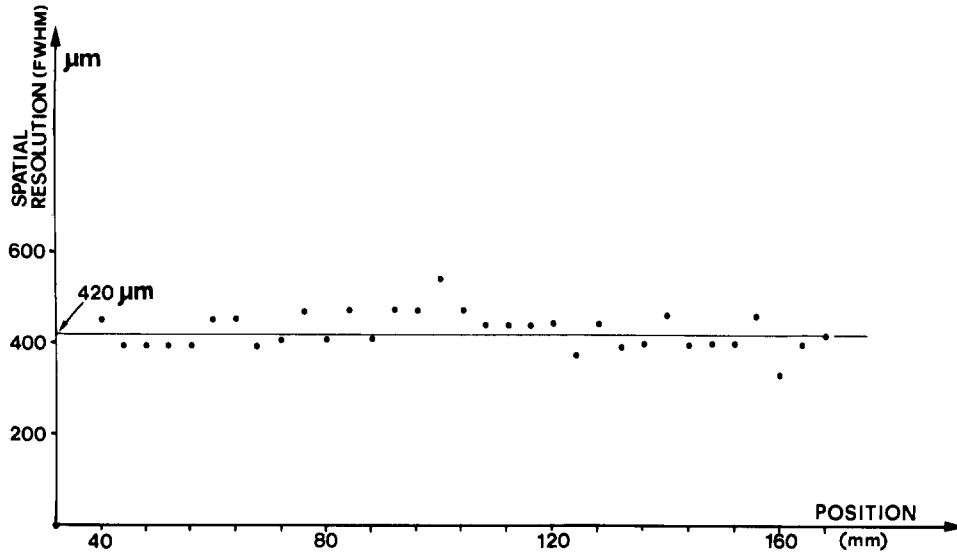
Fig. 6. Individual and mean spatial resolution as a function of the distance along the delay-line.

ing distribution from all the anode wires "lighted" by the source has a fwhm of 10 mm, which is in very good agreement with the predicted value obtained integrating along the x direction the density distribution $\rho(r)$ corresponding to the eq. (1) for a low energy, uncollimated γ-source with point-like ionization.

The measured spatial resolution is quite constant (± 50 μm) over the whole detector as one can see from fig. 6 showing the individual and the mean spatial resolution as a function of the position.

The linearity of the system has been tested moving an [55]Fe source along the y direction and recording the position of the peaks which correspond to different anode wires. Fig. 7 shows the delay time as a function of the position of the source. The data can be fitted by a straight line whose slope is the specific delay (τ) of the
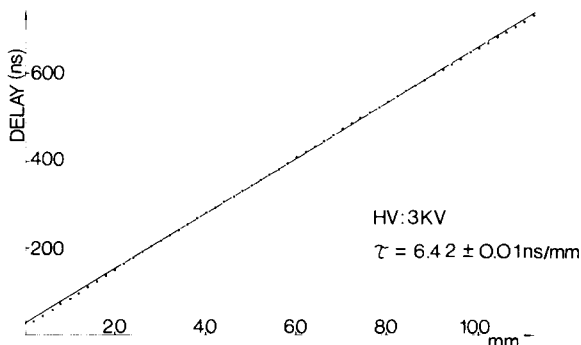

Fig. 7. The linearity of the read-out system, as measured by moving an [55]Fe source across the chamber. The slope is 6.42 ± 0.01 ns/mm.

delay-line, while the accuracy in determining the slope is a measure of the read-out system linearity ($\tau = 6.42 \pm 0.01$ ns/mm).

The spatial resolution for [14]C β^- rays (fig. 8) is strongly dependent on the extension of the ionization track associated with any individual electron emitted by the source ($E_{max} = 156$ keV). Many wires can be hit by the multiple avalanches produced by a single track. In this case the arrival time distribution from a single wire spreads out (fwhm $\simeq 1.5$ mm) in comparison with the corresponding value for the low energy X-rays. On the other hand the measured distribution from all the wires is now narrower (fwhm $\simeq 8$ mm).

To measure the resolving power of the system, i.e. the capability of identifying individual spots of β^- radioactivity, we have reconstructed the positions of two individual ^{14}C sources, 2 mm in diameter, 20 mm apart. The profile of a section through the center of the sources (fig. 9) has a fwhm $\simeq 4.7$ mm. Taking into account the finite dimension of the sources, we can set the resolving power of our system for ^{14}C sources at 4–4.5 mm, in good agreement with the predicted value from eq. (1). Furthermore, the area I on the detection plane "lighted" by a point-like source can be estimated $\simeq 60$ mm^2.

The overall efficiency for a ^{14}C source, i.e. the ratio k between the number of β^- rays detected by the chamber and the number of those leaving the source, has been measured $\simeq 0.2$, and can be factorized as:

$$k = f_\Omega f_T \eta_{MWPC}, \tag{2}$$

where f_Ω is the solid angle factor, f_T is the transmission factor of the β^- spectrum and η_{MWPC} is the detection
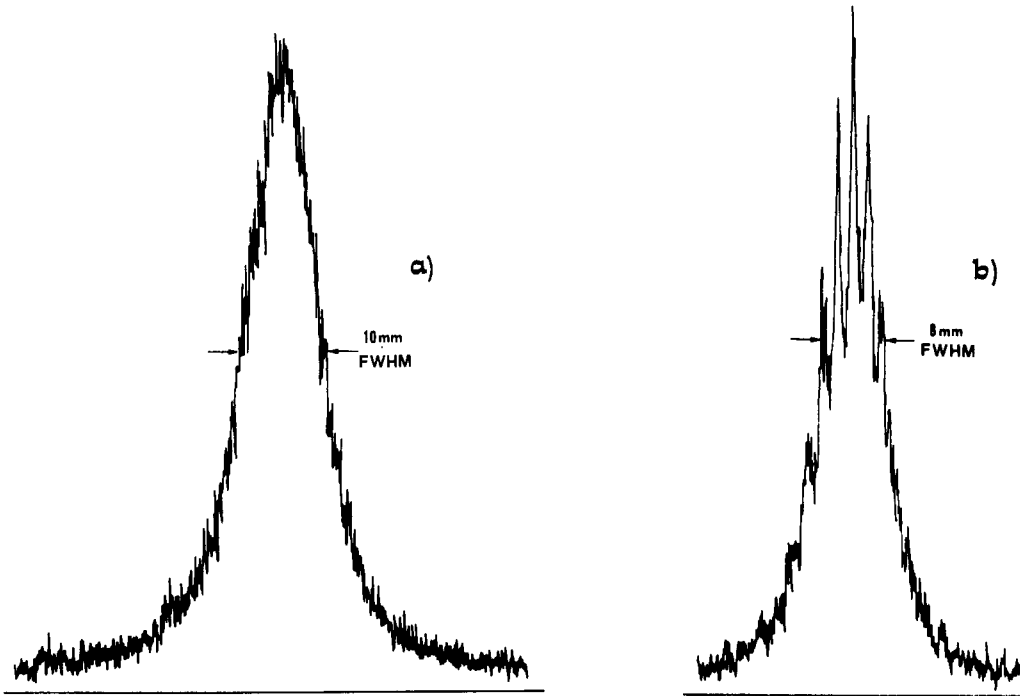
Fig. 8. Spatial resolution with ^{14}C β^- rays: a) x-coordinate, b) y-coordinate.

efficiency of the chamber at the working threshold. If $f_\Omega = 0.5$ and f_T is calculated at 0.7 we may derive from eq. (2) that the intrinsic efficiency of the MWPC $\eta \simeq 0.6$,

integrated over the energy spectrum of the transmitted β^- particles.

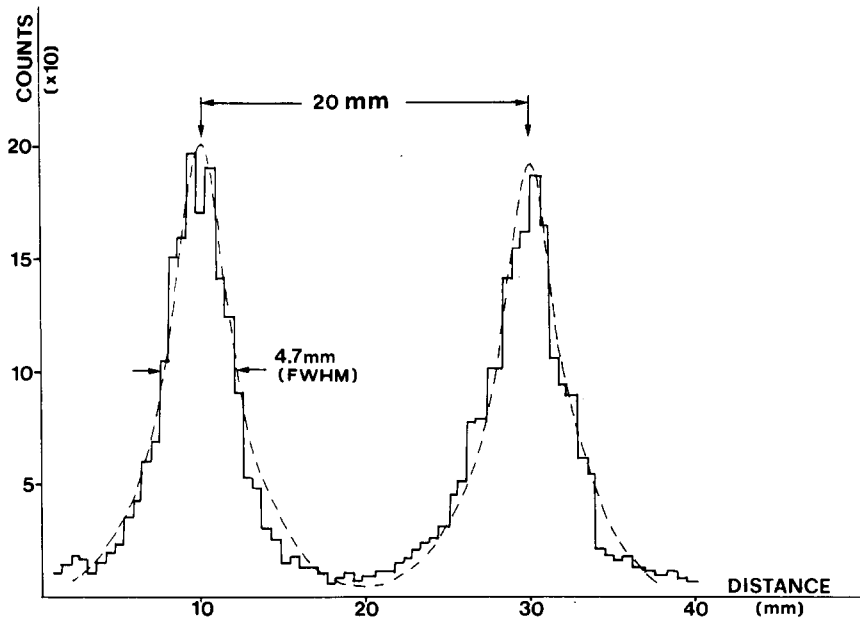The measured level of noise density is $N \simeq 10^{-4}$

Fig. 9. Full line: profile of a section through the center of the reconstructed image of two ^{14}C sources, 20 mm apart at $L = 5.3$ mm; dashed line: the corresponding theoretical distribution for two point sources obtained from eq. (1).
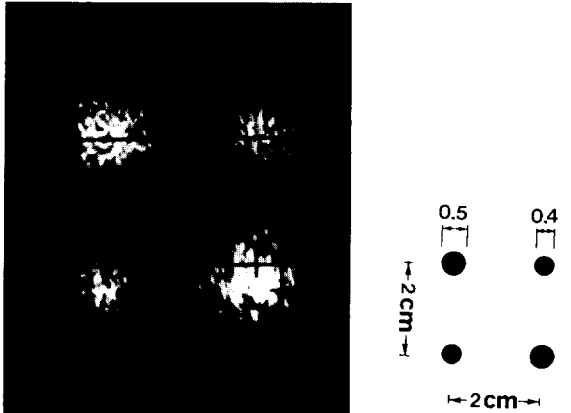
Fig. 10. Reconstructed map of four cell aggregates, each 2 cm apart and with 4×10^{-1} Bq/mm^2 activity density.

Fig. 11. Optical densitogram of a section through the cells on the righthand side of the picture of fig. 10.

cps/mm^2. If we define the sensitivity S(Bq/mm^2) of the detection system as the activity density of a source which gives a counting rate density equal to the noise level, then we can say, taking into account the overall detection efficiency and the source image spread-out, that $S \simeq NR/k$, where $R \sim [A + I + 2(AI)^{1/2}]/A$ is the ratio between the image and actual area A of the source. For a 1 mm^2 source, numerically $R \simeq I$ and $S \simeq NI/k \simeq 3 \times 10^{-2}$ Bq/mm^2. This result, which is quite adequate for our purposes can be further improved if extended sources are considered. In this case, indeed, R tends toward one, i.e. almost all the detected events are collected on a region not much wider than the actual source area. An activity density much lower can then be measured for extended source configuration. A sensitivity of $(0.3-3) \times 10^{-2}$ Bq/mm^2 may be foreseen for biological experiments with aggregates of mammalian cells.
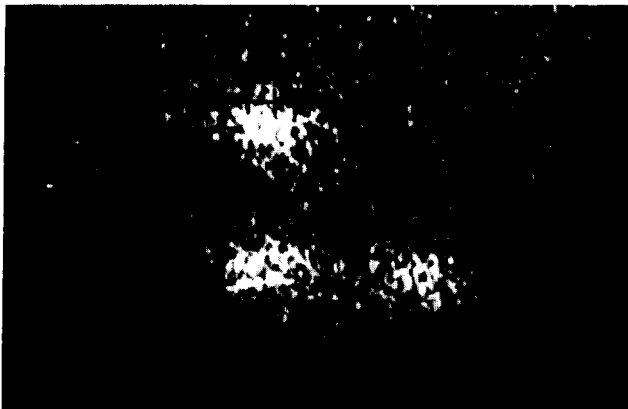
4. Imaging of cell colonies

The proposed biological experiment procedure has already been described [1]. In short, cells of human origin (HeLa) are seeded into "pretri dishes" in the presence of a nutrient medium. After a couple of weeks, hydroxyurea, a substance which specifically inhibits DNA replication but not repair synthesis, is added to the cultured cells, which are then exposed to UV light ($\lambda_0 = 260$ nm). A radioactive precursor of DNA synthesis, such as ^{14}C-thymidine, is added to the culture and, after an appropriate labelling time (a few hours), the residual ^{14}C-thymidine is washed out. Since DNA replication is almost completely blocked by the inhibitor, the radioactive precursor will mainly be utilized by the cells engaged in the repair of the DNA damaged by the UV-treatment.

Fig. 10 is a map, as reconstructed with the MWPC, of four living cell aggregates obtained with this procedure. Their relative distance is 2 cm and the active area is 12 or 19 mm^2. The activity density of each aggregate, as measured with a liquid scintillator technique, is $\simeq 4$

Fig. 12. Reconstructed map of three cell aggregates, 2 cm apart and with 1×10^{-1} Bq/mm^2 activity density. The fourth aggregate in the top right-hand corner is made of non UV-damaged, hence non-repairing, cells: its image is a simulation of the expected radioactivity background in a "mutant cell" colony.
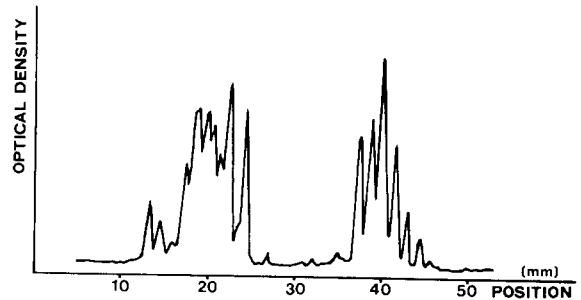
$\times 10^{-1}$ Bq/mm^2. Fig. 11 is the optical densitogram of a section through the cells shown to the right of fig. 10. In fig. 12 a similar map is shown, but the activity density is now $\simeq 1 \times 10^{-1}$ Bq/mm^2. The cells in the top right-hand corner of the picture were not exposed to UV light and simulate the expected background activity in a non repairing colony.

5. Conclusions

We have shown that a MWPC is a very useful detection system for the biological experiment outlined. Resolving power, linearity and sensitivity are good enough to permit the construction of biological maps of ^{14}C-labelled living cells that have a typical activity density of 100 mBq/mm^2 and ~ 1 cm separation. Further improvement can be obtained digitalizing the whole system, which allows for off-line analysis and data reduction.

Reference

[1] R. Bellazzini, A. Del Guerra, M.M. Massai, M. Ragadini, G. Spandre and G. Tonelli, Nucl. Instr. and Meth. 190 (1981) 627.